Relative abundances of novel cyclic prodelphinidins in wine depending on the grape variety

Edoardo Longo[a], Vakare Merkyte[a], Fabrizio Rossetti[b], Pierre-Louis Teissedre[c], Michael Jourdes[c], Emanuele Boselli[a,*]

AFFILIATION

[a]Free University of Bozen-Bolzano, Faculty of Science and Technology, Piazza Università 5, Bozen-Bolzano, 39100 Bozen-Bolzano, Italy

[b]Università Politecnica delle Marche, Department of Agricultural, Food and Environmental Sciences, Via Brecce Bianche, 10, 60131 Ancona, Italy

[c]University of Bordeaux, Unité de recherche Œnologie, EA 4577, USC 1366 INRA, ISVV, 210 Chemin de Leysotte, 33882 Villenave d'Ornon cedex, France

*corresponding author:

Prof. Emanuele Boselli (ORCID ID: 0000-0001-7931-6961)

Address: 4

E-mail: emanuele.boselli@unibz.it

phone: +390471017217

This article has been accepted for publication and undergone full peer review but has not been through the copyediting, typesetting, pagination and proofreading process which may lead to differences between this version and the Version of Record. Please cite this article as doi: 10.1002/jms.4280

Abstract

The identification of cyclic B-type procyanidins in grape and wine was recently disclosed. Some of these were also found in berries of totally different vegetal species (e.g. *Vaccinium* sp.). However, presence of a wider class of these cyclic condensed tannin compounds with variably substituted monomers has never been addressed so far. Here, an extended list of oligomeric cyclic proanthocyanidins (PAC) bearing variable substitution patterns on the main flavan-3-ol unit has been searched in wines. Nearly 7,600 theoretical structures were calculated and searched in red and white wine samples made from different grape varieties. Moreover, an hydrogen/deuterium exchange approach (already applied to a cyclic tetrameric procyanidin) coupled to high-resolution mass spectrometry was applied to confirm their cyclic B-type structure rather than a non-cyclic A-type structure, otherwise isomeric and undistinguishable by LC-MS alone. The main group of novel cyclic PAC observed is shown to contain (epi)gallocatechin beside (epi)catechin as the constituent monomers.

Keywords: cyclic procyanidins; cyclic prodelphinidins; crown proanthocyanidins; high resolution mass spectrometry; wine authenticity.

Abbreviations

a- = non-cyclic A-type; afz = (epi)afzelechin; c- = cyclic B-type; CH3 = (epi)gallocatechin-*O*-CH_3; CHP, cyclic hexameric proanthocyanidin; Cp = Chardonnay Passito Aurum; CPP, cyclic pentameric proanthocyanidin; CTP, cyclic tetrameric proanthocyanidin; EIC, extracted ion chromatogram; gallate = (epi)catechin gallate; galloc = (epi)gallocatechin; l- = non-cyclic B-type; LHP, linear (non-cyclic) hexameric proanthocyanidin; LOD, limit of detection; LPT, linear (non-cyclic) pentameric proanthocyanidin; LTP, linear (non-cyclic) tetrameric proanthocyanidin; PAC, proanthocyanidins; PC, procyanidins; PCA, Principal Component Analysis. Abbreviations for the wines: L = Lagrein, LP = Lagrein Prestige, LE = Lagrein Eyrl, LG = Lagrein Grieser, CF = Cabernet Franc, CS = Cabernet Sauvignon, MC = Merlot collection, MB = Merlot barrique, BB = Blauburgunder, SMM = St.Magdalener Moar, SMH-1 = St.Magdalener Huck-1, SMH-2 = St.Magdalener Huck-2, GK = Gewürztraminer Kleinstein, G = Gewürztraminer, GP = Gewürztraminer Passito, SB-1 = Sauvignon blanc-1, SB-2 = Sauvignon blanc-2.

Introduction

Proanthocyanidins, known also as condensed tannins, are one of the most important secondary metabolite families in grape skins, grape seeds and in wine. Proanthocyanidins are oligomeric and polymeric structures built-up with flavan-3-ol monomers, such as (+)-catechin and (−)-epicatechin.[1] However, beside (+)-catechin and (−)-epicatechin, a large variety of substituted flavan-3-ol sub-units has been identified in grapes' and wines' proanthocyanidins. For example, galloylated flavanols such as (–)-epicatechin gallate,[2] and (+)-catechin gallate were identified in grape seeds.[3]

Prodelphinidins are polymeric structures containing (epi)gallocatechin and commonly observed in grape skin from *Vitis vinifera* varieties,[4] while the presence of (+)-gallocatechin-3-*O*-gallate was reported in non-*Vinifera* grape varieties.[5] Furthermore, glycosylated flavan-3-ols were observed in grapes extracts and wine by mass spectrometry.[6] More recently, (–)-epicatechin units esterified with vanillic acid ((–)-epicatechin-3-*O*-vanillate) have been identified and characterised in grape seeds and red wines.[7]

Condensed tannins identified in wine grape seeds have been found by HRMS and MS/MS to possess a degree of polymerization (DP) and galloylation (DG) up to 20 and 11 respectively, with molecular masses reaching up to 6067 Da.[8]

The discovery of unconventional cyclic procyanidins (referred as crown procyanidins) in wines from the Bordeaux region (France) has been disclosed in a series of reports aimed at attesting their structure and their distribution in red wines.[9,10] In Jouin et al. (2017), the NMR resolved structure of the crown tetramer (CTP) was presented. More recently, an H/D isotope exchange approach coupled to HPLC-HRMS/MS was employed to confirm the structure of a crown tetrameric procyanidin (CTP).[11] However, the use of H/D isotope exchange was applied to solve an unforeseen ambiguity: these cyclic novel procyanidins share the same elemental composition with previously known non-cyclic analogues, namely the A-type (they are isomeric). Instead, these new compounds proposed were all cyclic B-type ones. The difference between these two classes is the presence of one or more inter-monomer (monomer *n* to monomer *n*-1) C-O-C bonds in the A-type structure *vs* a single inter-monomer head-tail C-C bond –the *n* monomer to the initial monomer - in the cyclic B-type structure. In the latter, this C-C bond is virtually in place of two C-H bonds present in the more typical non-cyclic B-type. An example is shown in **Figure 1**. The species in **Figure 1-A** and **1-C** present only one structural difference useful to distinguish them by an LC-MS approach, namely the number of exchangeable phenolic protons in the two isomers, which differ by one unit. The H/D isotope exchange approach allowed counting these exchangeable protons, whose number differentiates the two isomeric classes unambiguously. In fact, the H/D replacement indicated that the main $C_{60}H_{48}O_{24}$ compound observed was of B-type (**Figure 1-C**),[11] thus confirming the previous observations.[9,10] The method allowed to identify correctly also the isomeric non-cyclic A-type procyanidins in a peanut skin extract.[12]

Furthermore, the distribution of these species (cyclic tetrameric, pentameric and hexameric procyanidins - CTP, CPP and CHP, respectively) in many wines obtained from different grape varieties was investigated, showing that their proportions over the total amount of procyanidins (by number of monomer units) was related to the specific grape variety and to the winemaking procedure.[13] However, in the cited work, only the flavan-3-ols constituent (+)-catechin and (−)-epicatechin monomer units were addressed. Consequently, it can be considered that the list of crown proanthocyanidins might be much longer than the one initially investigated. In fact,

beside (+)-catechin and (−)-epicatechin, many more possible monomer units with different substitutions should be considered for building up the wide proanthocyanidins class, as for example (epi)gallocatechin, (epi)catechin gallate, (epi)afzelechin and *O*-mono- or di-methylated (epi)gallocatechins (the latter ones are not actually present in grape) like observed with linear proanthocyanidins in wine, grapes and other plant sources (**Figure 2**).[1,4] Besides, potassium and calcium complexes of non cyclic and cyclic B-type proanthocyanidins were recently discussed in relation with their relative isomeric abundances in wines.[14]

Therefore, our aim was to investigate the presence of possible natural cyclic oligomers in wine samples containing these monomer units, exploiting the aforementioned H/D exchange approach for confirmation. Overall, this method could not yield structural details of the C-C inter-flavanol bonding (e.g. $C_{n-1}4$-C_n6 or $C_{n-1}4$-C_n8), nor the configuration of the stereogenic centers (e.g. (+)-catechin or (-)-epicatechin), which would still require NMR or crystal X-rays crystallography for resolution. However, the present approach allowed to unambiguously indicate whether a compound was of the cyclic or linear type. This information was not provided unambiguously only by HPLC-HRMS/MS and it would support the NMR results. The first step was to consider all possible variations (e.g. (epi)gallocatechin gallate), for simplicity up to a maximum of two modifications, from the (epi)catechin model structure. Then, the presence of A-type or B-type bonds was considered. A-type bonding is theoretically possible up to *n*-1 times *per* molecule (where *n* = number of constituent monomer units) whereas the additional B-type bond could be only one *per* molecule. Taken these considerations into account, a list of nearly 7,600 theoretical proanthocyanidins (PAC) compounds (data available on request) was built up to the hexamers (only for non-redundant and plausible species). A parallel list was built for the deuterium substituted species, where only the exchangeable O-H bonds were replaced with correspondent O-D bonds. This allowed to distinguish the theoretical A-type PAC (with at most one A-linkage) from the cyclic B-type PAC, since they are not isomeric anymore, as proved in a recent report.[11] For the resolution of this theoretical enormous number of possible species, a HPLC-HRMS/MS method was employed. All the detected, identified and confirmed species (by MS/MS and/or by H/D exchange) are presented. Fragmentation patterns were recorded for distinguishing possible contributing isomers. Monomer unit fragments in the oligomer MS/MS spectra were carefully exploited for excluding

possible regio-isomers that could not be discriminated by HRMS only. In a recent report, the use of the cyclic to total PAC peak area ratios, combined with other variables (e.g. spectrophotometric and chromatographic) provided a useful tool for discriminating wines on the basis of the grape variety.[13] This new investigation is aimed at extending the knowledge of these new cyclic species and at providing an improved tool for discriminating wine types by grape variety and winemaking procedures.

Experimental

Materials

Solvents and pure reagents (at LC-MS grade) were obtained from Sigma-Aldrich Ltd, as well as deuterium oxide (D_2O) (99.9% D). White and red wines are those reported by Longo *et al*.[13] All the wines were produced during the harvest 2016 and were donated by a local cooperative winery (Kellerei Bozen, BZ, Italy) and a local agricultural high school (Happacherhof, Auer/Ora, BZ, Italy). All wines were PDO/DOC grade from the South Tyrol region. For simplicity, wines (with their abbreviation) are listed in **Table 1**.

Samples preparation

The wine samples were prepared according to a published report.[11] Briefly, wines were concentrated at 30^{o}C at reduced pressure followed by 30 min of gentle N_2 flux, then they were re-diluted to a final concentration 10 times higher than the starting sample. For MS/MS studies the re-dilution was limited to provide a concentration 10 to 30-times higher. When H/D exchange was performed, the samples were first dried and recovered 3 times in pure deuterium oxide before fluxing N_2 and recovering them in the fully deuterated mobile phase A. The samples were filtered (0.2 µm, regenerate cellulose) before HPLC injection.

HPLC-HRMS/MS analysis

The HPLC-HRMS/MS method applied was adapted from published reports.[11-15] The HPLC-HRMS system used consisted of a Q Exactive HRMS instrument (Thermo Fisher Scientific, Waltham, MA, USA) coupled to an Agilent 1260 HPLC (Agilent Technologies Santa Clara, CA, USA) with a 16 channel DAD detector. The separation was carried out with a ODS Hypersyl C18 LC column (125 mm × 4.6 mm

i.d., 5 µm, Thermo Sci.) protected with a HPLC pre-column filter (ODS Hypersil, 5 µm pore size, 10 x 4 mm drop-in guards, Thermo Fisher Scientific). The HPLC flow rate was 1 mL min^{-1}. The mobile phase consisted of solvent A (0.1% v/v formic acid in 0.02 mol L^{-1} ammonium formate in water or 0.1% v/v deuterated formic acid in 0.02 mol L^{-1} fully deuterated ammonium formate in D_2O) and B (0.1% v/v formic acid in saturated ammonium formate acetonitrile or 0.1% v/v deuterated formic acid in fully deuterated saturated ammonium formate acetonitrile. The gradient was set as follows: from 5% (v/v) B at 0 min to 25% B (v/v) at 21 min, then to 95% B at 22 min until 27 min, to 5% at 28 min, followed by a re-equilibration step (5% B) at 32 to 35 min. The DAD spectra were recorded from 210 to 600 nm and provided real-time monitoring at 280 nm, 320 nm, 365 nm, 420 nm and 520 nm (+/- 4 nm) to identify the main phenolic compounds of the wines for further studies. A post-column flow splitter was used to feed both analyzers in parallel (DAD and HRMS) at a fixed ratio. For full MS analysis, the mass spectrometer heated ESI source was operated in positive ionization mode using the following conditions: sheath gas at 20 (arbitrary units), aux gas at 5 (arbitrary units), aux temperature 250°C, spray voltage at +3,500 kV, capillary temperature at 320°C and RF S-lens at 70. The mass range selected was from *m/z* 500 to 2,000 with a FullMS set resolution of 70,000 (@200 *m/z*), AGC target at $3 \cdot 10^6$, max injection time of 300 ms. The LC-HRMS/MS experiments were run according to the following settings: Full-MS parameters were kept as shown, MS/MS AGC target 10^6, max. injection time 300, FT-MS set resolution 35,000, loop count 5, isolation window 2 or 3 m/z with 1 m/z offset, normalized collision energy 15 eV. For data dependent settings: minimum AGC target $3 \cdot 10^3$, apex trigger 2 to 8 sec, charge exclusion 3 – 8 and higher, dynamic exclusion 3 sec, “if idle” tool set to “pick others”. Lock masses were constantly employed to correct mass deviations across the Full MS acquisition range throughout the experiments. When D_2O was employed, the lock masses were modified accordingly into the main instrument method. The HPLC-DAD data (only of the non re-concentrated wine samples) were collected and analyzed by OpenLab software while the MS data and results were collected and analyzed by Xcalibur 3.1 software and Compound Discoverer 2.0 (Thermo Scientific).

Statistical analysis

XLStat (version 2016.02.28430, Addinsoft, Paris, France) and The Unscrambler (version 10.4.43636.111, CAMO Software AS., Oslo, Norway) software were employed for the statistical analysis

Results and discussion

In **Table 2** the list of PAC species identified is reported. The analysis was aimed mainly at all the PAC between the dimeric and the hexameric oligomers. The main limitations encountered for the analysis were (a) the low chromatographic separation between the peaks due to the extremely high number of species; (b) the ten-times reconcentration applied with respect to wine; (c) the high number of isomers for most of the species and (d) the low intensities for some identified species. Consequently, only those compounds that were eventually confirmed are reported in **Table 2**.

The spectra obtained by means of HRMS in H_2O, tandem MS in H_2O and HRMS in D_2O are shown in **Supporting Information** (**Figures SI 1-24**) for the compounds listed in **Table 2**. The presence of (epi)catechin-*O*-gallates and (epi)catechin hydroxybenzoates was observed for dimers and trimers.[16] However, our approach did not allow to assign unambiguously the hydroxybenzoate ester compound: an isomeric theoretical compound (in both water and deuterium systems) is the l-dimer (linear) with one (epi)afzelechin and one (epi)afzelechin-*O*-gallate (called l-dimer-2-afz-1-gallate). The MS/MS spectrum showed the fragment *m/z* 139.038 (**Figure SI 6E** in the **Supporting Information**), which is compatible with both the hydroxybenzoic acid-related cation and/or the derived fragment from gallic acid after loss of two oxygens, namely [gallic acid - 2O + H]$^+$. In addition, also the gallic acid-related ion *m/z* 151.038 was present. However, the second hypothesis (the presence of gallate and not hydroxybenzoate) would imply that the *m/z* 699.169 precursor must not contain any (epi)catechin (because its exact mass should be higher in such instance). However, the *m/z* 289.070 fragment (usual MS/MS catechin fragment) was present, therefore the assignment was not feasible. Only an MS^3 analysis could have helped, but considering that the work aimed at a different objective, we postponed its resolution to future investigation.

The main goal was the identification and confirmation (by means of H/D exchange and MS/MS comparisons) of new crown procyanidin- analogs with monomers different from (epi)catechins.

Indeed, the main constituents of PAC from the tetramers up to the hexamers were (epi)catechin and (epi)gallocatechin units (prodelphinidins) (as expected), since their monomer compounds are known to be the most abundant in grape and wines.[17]

In detail, the fragmentation preferences for PAC containing (epi)gallocatechins were analogous to those of the previously seen procyanidins ((epi)catechins only): the cyclic forms (**Figure SI 14** and **Figure SI 20**) have the tendency of fragmenting less than their linear counterparts in the conditions applied.[11] In these cyclic B-type forms, the loss of OH units occurred before the loss of entire monomers, whereas the linear ones displayed more intense fragments (with a much lower pseudo-molecular ion intensity) with a smaller relative contribution from OH losses. As mentioned in the previous reports, the increased resistance of the cyclic backbone of these novel PAC is a peculiar feature to distinguish the cyclic B-type PAC from the non-cyclic ones (B- or A- type alike).

A-type PAC were also observed up to the trimeric stage (e.g. a-dimer, a-dimer-1-galloc, a-trimer and a-trimer-1-galloc along with methylated analogs). It was also noticed that cyclic B-types with PAC less than four units were absent. Regarding the confirmed PAC (**Table 2**), the composition was limited almost only to (epi)catechins and (epi)gallocatechins. Nonetheless, these are the most abundant flavan-3-ols in wine according to the literature.[17]

As previously seen by Longo et al.[11-14] here too, the c-analogs appear to retain those features that distinguished them from their linear analogs, namely (a) the anticipated retention times and (b) the lower number of peaks (even just one). It was already reported that the increased polarity, a lower fragmentation probability (along with all the differences in the fragmentation patterns) and fewer peaks (usually only a main one with much smaller traces at higher retention times) are features distinguishing the cyclic from their linear (a- or l-) counterparts.

In order to obtain a fingerprint of the crown prodelphinidins in wines, we applied the same procedures shown earlier.[13] Briefly, the integrated relative abundance of these new cyclic structures was divided by the sum of the linear and cyclic analogs, from tetramers to hexamers. The results are shown in **Figure 3**.

As seen earlier for PAC without (epi)gallocatechins,[13,14] a dependence is present over the grape variety as shown with ANOVA (**Table SI 1**, **Supporting Information**). At the same time, the PCA run on these observations, using only these four variables, explained 100% of the variance (see PC1 *vs* PC2 and PC1 *vs* PC3 in **Figure SI 25** and **Figure SI 26** in **Supporting Information**).

Unsurprisingly, the major effect was given by the comparison of wines obtained with red *vs* white grape varieties. The amount of PAC in red wines was one order of magnitude higher than in white wines. However, as it was seen previously for PAC without (epi)gallocatechins,[13,14] the calculated ratios carry much more information. Red and white wines showed increasing proportions of the cyclic analogs (from 4 to 6 units) towards heavier PAC (while the overall PAC abundance decreased). It has been previously suggested that this effect (the increasing proportions of cyclic at higher oligomeric stages up to the hexamer) may be a consequence of a higher cyclization probability, which may be increasing when approaching six-term oligomers. Another possible explanation might be a parallel loss of non-cyclic PAC at higher oligomeric stages due to reduced solubility and consequent precipitation.

In white wines, the relation between chain lengths and cyclic proportions seems to be more complex. As seen previously, the cyclic proportion varied greatly with the grape variety. Here, the Gewürztraminer and Sauvignon blanc seemed to possess much less or even absent c-tetramer-1-galloc than l-tetramer-1-galloc, whereas this proportion was higher than 80% in Chardonnay (Cp sample, a Passito wine). The c-pentamer-1-galloc instead was completely absent in Gewürztraminer, but was very much higher in Sauvignon blanc and Chardonnay. Overall, this allowed to distinguish the wines efficiently by their own grape variety as confirmed by ANOVA (**Table SI 1**).

Conclusions

The presence and distribution of cyclic B-type proanthocyanidins containing (epi)gallocatechins (i.e., prodelphinidins) in red and white wines have been demonstrated for the first time. Previous evidences of the relation between these cyclic oligomers and other factors (e.g. winemaking procedures) were already shown for procyanidins.[12] Overall, these two classes (cyclic B-type procyanidins and cyclic B-type prodelphinidins) showed similar behaviors under many respects: *(a)* the retention times were anticipated with respect to their linear analogs; *(b)* they showed much fewer HPLC peaks with respect to their linear analogs, indicating the presence

of just one main regio- and stereoisomer; *(c)* the MS/MS spectra showed much less fragmentation with respect to their linear analogs (higher pseudo-molecular ion intensity) at 15 eV collision energy.

In conclusion, this work has extended the reach of previous efforts undertaken for understanding the nature and distribution of these novel proanthocyanidins in white and red wines. This work also confirmed their structure as cyclic B-type PAC by applying hydrogen/deuterium exchange. Notably, cyclic PAC with monomers other than (epi)catechins were unknown so far. Besides, the proportion of cyclic species *vs* the total amount (*per* number of monomeric units) was yet again greatly affected by the grape varieties in wine. Further efforts ought to be put forward to enhance the method for screening less abundant cyclic proanthocyanidins, which might have been overlooked for the explained reasons or even completely missed, as well as for higher molecular weight PAC (furtherly substituted hexamer, heptamers etc.). Furthermore, the cyclization ability should be rationalized in terms of flavan-3-ol ring substitutions, initial monomers concentration, PAC solubility, chain length and conformations. However, based on the experiments done so far, the usefulness of the H/D exchange approach applied to HRMS analysis of PAC was again proved as a complementary tool to tandem MS and NMR structural resolution. Besides, the dependence of cyclic proanthocyanidins distribution upon the grape variety was again confirmed and proved to be a promising tool for wine authenticity and quality assessment.

Acknowledgement

The author thanks Provincia di Bolzano (Italy) for the financial support (Landesregierung Beschluss Nr. 1472, 07.10.2013) and the Camera di Commercio di Bolzano for networking and support.

Conflict of interests

The authors declare no conflict of interests.

References

1. Lin LZ, Sun J, Chen P, Monagas MJ, Harnly JM. UHPLC-PDA-ESI/HRMS^n profiling method to identify and quantify oligomeric proanthocyanidins in plant products. *J Agric Food Chem.* 2014;*62*(39):9387-9400.
2. Su CT, Singleton VL. Identification of three flavan-3-ols from grapes. *Phytochemistry.* 1969;8(8):1553-1558.
3. Lee CY, Jaworski A. Phenolic compounds in white grapes grown in New York. *Am J Enol Viticult.* 1987;38(4):277-281.
4. Chira K, Schmauch G, Saucier C, Fabre S, Teissedre PL. Grape variety effect on proanthocyanidin composition and sensory perception of skin and seed tannin extracts from Bordeaux wine grapes (Cabernet Sauvignon and Merlot) for two consecutive vintages (2006 and 2007). *J Agric Food Chem.* 2009;57(2):545-553.
5. Lee CY, Jaworski AW. Identification of Some Phenolics in White Grapes. *Am J Enol Viticult.* 1990;41(1):87-89
6. Delcambre A, Saucier C. Identification of new flavan-3-ol monoglycosides by UHPLC-ESI-Q-TOF in grapes and wine. *J. Mass Spec.* 2012;47(6):727-736.
7. Ma W, Waffo-Teguo P, Jourdes M, Li H, Teissedre PL. First evidence of epicatechin vanillate in grape seed and red wine. *Food Chem.* 2018;259:304-310.
8. Ma W, Waffo-Téguo P, Paissoni MA, Jourdes M, Teissedre PL. New insight into the unresolved HPLC broad peak of Cabernet Sauvignon grape seed polymeric tannins by combining CPC and Q-ToF approaches, *Food Chem.* 2018;249:168-175.
9. Jouin A, Rossetti F, Teissèdre PL, Jourdes M. Evaluation of crown procyanidins contents in different variety and their accumulation kinetic during grape maturation. In 10th In Vino Analytica Scientia (IVAS) Symposium, 17-20 July 2017, p. 160, Salamanca, Spain. Salamanca.
10. Jourdes M, Zeng L, Pons-Marcadé P, Rivero Canosa M, Richard T, Teissèdre PL. A new procyanidin tetramer with unusual macrocyclic skeleton from grape and wine. In 39' World Vine and Wine Congress - Theme 2 Oenology, p. 432-433, 24-28 October 2016, Bento Gonçalves, Brazil.
11. Longo E, Rossetti F, Scampicchio M, Boselli E. Isotopic exchange HPLC-HRMS/MS applied to cyclic proanthocyanidins in wine and cranberries. *J. Am. Soc. Mass Spec.* 2018;29(4):663-674.

12. Longo E, Rossetti F, Merkyte V, Boselli E. Disambiguation of isomeric procyanidins with cyclic B-type and non-cyclic A-type structures from wine and peanut skin with HPLC-HDX-HRMS/MS. *Under editorial revision.*
13. Longo E, Rossetti F, Jouin A, Jourdes M, Teissedre PL, Boselli E. Distribution of cyclic hexameric proanthocyanidin and its tetrameric and pentameric congeners in red and white wines. *Under editorial revision*.
14. Longo E, Rossetti F, Merkyte V, Obiedzińska A, Boselli E. Selective binding of potassium and calcium ions to novel cyclic proanthocyanidins in wine by HPLC-HRMS, *Rapid Commun Mass Sp* 2018, in press, https://doi.org/10.1002/rcm.8221
15. Savini S, Loizzo MR, Tundis R, Mozzon M, Foligni R, Longo E, Morozova K, Scampicchio M, Martin-Vertedor D, Boselli E. Fresh refrigerated *Tuber melanosporum* truffle: effect of the storage conditions on the antioxidant profile, antioxidant activity and volatile profile. *Eur Food Res Technol.* 2017;243(12):2255–2263.
16. Osanai K, Huo C, Landis-Piwowar KR, Dou QP, Chan TH. Synthesis of (2R,3R)-epigallocatechin-3-*O*-(4-hydroxybenzoate), a novel catechin from *Cistus salvifolius*, and evaluation of its proteasome inhibitory activities. *Tetrahedron.* 2007;63(32): 7565–7570.
17. Monagas M, Bartolomé B, Gómez-Cordovés C. Updated knowledge about the presence of phenolic compounds in wine. *Crit Rev Food Sci Nutr.* 2005;45:85–118.

Table 1. List of wines studied (with commercial names).

Wine sample	Abbreviation
Lagrein	L
Lagrein Prestige Klebelsberg	LP
Lagrein Eyrl	LE
Lagrein Grieser Collection I	LG-1
Lagrein Grieser, Collection 2	LG-2
Cabernet Franc	CF
Cabernet Sauvignon	CS
Merlot collection	MC
Merlot barrique	MB
Blauburgunder (Pinot noir)	BB
Blauburgunder (Pinot noir)	BB-rep
St.Magdalener Moar	SMM
St.Magdalener Classico Huck-I	SMH-1
St.Magdalener classico Huck-II	SMH-2
Gewürztraminer Kleinstein	GK
Gewürztraminer	G
Gewürztraminer Passito	GP
Sauvignon Blanc	SB-1
Sauvignon Blanc	SB-2
Chardonnay Passito Aurum	Cp

Table 2. List of found PAC species identified and confirmed.

PAC species (*)	detected EIC peaks	found ion (m/z)	av. Δ m/z (ppm)	related deuterated ion (m/z)	retention times in H_2O (±0.1 min)	retention times in D_2O (±0.1 min) (***)	comment	MS/MS fragments with H_2O	r.t. of MS/MS (min)
a-dimer (**Figure SI 1**)	> 10	577.1345	0.7	587.1969	2.8, 3.3, 4.0, 4.5, 5.3, 5.7, 7.6, 8.5, 9.0, 9.8, 10.3, 11.3, 12.5, 12.9, 13.5, 14.0, 14.4, 14.7, 16.2, 16.8, 17.3, 18.0, 18.8, 19.8, 20.4, 23.0	8.5, 10.5, 11.2, 15.4,15.5, 17.8, 19.4, 19.7, 21.0, 23.7, 26.4	many isobaric peaks	NA	NA
l-dimer (**Figure SI 2**)	6	579.1497	0.0	590.2144	7.6, 9.6, 10.3, 13.3, 16.7, 23.8	8.5, 12.5, 13.5, 17.0, 17.3, 17.7		**579.149**, 427.102, 409.091, 301.070, 291.086, 289.070, 287.054, 275.054, 271.060, 247.060	7.6 (**)
a-dimer-1-galloc (**Figure SI 3**)	> 10	593.1288	-0.3	604.1970	3.7, 4.4, 5.3, 6.6, 7.2, 8.2, 8.3, 8.7, 9.2, 9.7, 10.0, 10.2, 10.5, 11.0, 11.4, 11.6, 12.0, 12.2, 12.9, 13.3, 14.0, 15.7, 16.6, 18.5, 21.9	5.3, 6.1, 7.5, 9.0, 9.2, 12.2, 13.1, 16.4, 19.4, 20.0, 20.8, 22.0, 22.5, 23.7	many isobaric peaks	NA	NA
l-dimer-1-galloc (**Figure SI 4**)	3	595.1446	0.0	607.2196	4.3, 5.3, 6.7	6.1, 11.2, 12.7	in D_2O peaks also at much later r.t., likely from fragmentation of other compounds	**595.144,** 443.097, 425.086, 317.065, 305.065, 291.086, 287.054, 275.054, 263.054	4.3 (**)
l-dimer-2-galloc (**Figure SI 5**)	4	611.1405	1.6	624.2238	2.5, 3.5, 4.3, 5.3, 7.8	1.0, 3.1	traces at later r.t.	NA (interfering compound at 611.18 m/z)	NA
l-dimer-2-afz-1-gallate	4	699.1690	-2.8	710.2423	12.7, 16.3, 16.6, 17.6	1.8, 6.5, 17.4, 18.2	many (weaker) isobaric peaks	**699.168**, 561.136, 547.123, 531.126, 495.127, 427.101, 411.106, 409. 409.090, 301.070, 289.070,	17.6 (**)

or l-dimer-1-(hydroxy-benzoate) (**Figure SI 6**)								287.054, 247.059, 211.168, 194.117, 163.038, 139.038, 127.039, 123.044, 121.028	
l-dimer-1-gallate (**Figure SI 7**)	> 4	731.1598	-1.2	744.2422	11.7, 12.3, 13.2, 20.0	8.5, 14.2, 15.7, 17.5, 21.3, 24.2	many isobaric peaks	**731.158**, 713.148, 605.127, 579.111, 563.116, 543.127, 443.095, 427.101, 409.090, 301.070, 289.070, 287.054, 275.054, 273.074, 271.060, 259.060, 247.060, 163.038, 153.017, 151.038	13.2 (**)
l-trimer (**Figure SI 8**)	> 10	867.2124	-0.8	883.3121	3.3, 8.2, 9.0, 9.8, 10.2, 10.8, 12.5, 12.8, 14.0 (…)	4.1, 5.5, 9.1, 9.4, 10.1, 10.8, 11.3, 12.0, 13.8 (…)	many isobaric peaks	**867.210**, 849.198, 715.164, 697.153, 579.148, 577.132, 559.122, 545.106, 451.100, 437.085, 427.101, 425.085, 409.090, 407.074, 291.085, 289.069, 287.054, 275.054, 271.059, 247.059, 245.043	12.9 (**)
l-trimer-1-galloc (**Figure SI 9**)	> 10	883.2072	-0.9	900.3118	2.1, 6.8, 7.2, 7.8, 8.2, 8.5, 9.7, 10.2, 10.9, 11.8, 12.5	2.7, 3.2, 8.3, 8.8, 9.7, 9.0, 9.3, 9.6, 9.7, 12.7, 13.1, 16.5	many isobaric peaks	**883.205**, 865.194, 731.158, 713.148, 697.154, 595.143, 593.127, 579.148, 577.094, 575.120, 467.096, 449.085, 437.085, 427.101, 425.085, 413.085, 409.090, 407.075, 305.064, 291.085, 289.070, 287.054, 275.054, 263.054, 247.060, 245.043	7.2 (**)
l-trimer-2-galloc (**Figure SI 10**)	8	899.2021	-0.8	917.3159	5.2, 5.6, 6.4, 7.3, 7.9, 8.5, 9.1, 9.7, 10.4	9.04	very weak in D_2O	**899.199**, 731.158, 609.121, 595.142, 443.080, 441.080, 423.070, 413.085, 347.074, 317.064, 305.064, 291.085, 287.053, 275.054, 263.054, 245.043	6.4 (**)
l-trimer-1-gallate (**Figure SI 11**)	> 10	1019.2236	-0.4	1037.3369	7.1, 8.3, 10.8, 10.9, 11.8, 13.0, 13.7, 14.4, 14.9, 15.7, 16.3, 16.9, 17.3, 18.4, 19.0, 19.6 (…)	4.0, 9.5, 11.8, 12.0, 13.6, 14.2, 14.8, 15.6, 17.4, 17.4, 17.9, 18.1, 18.2, 18.5, 18.8, 19.1	many isobaric peaks	**1019.220**, 867.172, 849.196, 731.157, 729.141, 697.154, 695.377, 679.139, 579.110, 577.094, 571.123, 559.121, 545.105, 541.110, 527.095, 517.111, 473.272, 441.080, 439.101, 411.105, 409.090, 407.074, 331.044, 303.048, 291.085, 289.070, 287.053, 271.059, 247.059, 245.043, 153.017	10.9 (**)

c-tetramer *(****)*	1	1153.2604	-0.3	1174.3909	3.7	5.0	traces at higher r.t. (probable a-type tetramer)	**1153.259**, 1001.213, 865.197, 695.140, 577.134, 451.102, 409.091, 289.070, 247.060	3.7
l-tetramer *(****)*	> 10	1155.2760	-0.7	1176.4075	6.3, 7.2, 7.5, 8.5, 9.2, 9.8, 10.8, 11.3, 12.7, 13.5, 14.7, 19.3 (…)	8.4, 8.7, 9.7, 10.2, 11.0, 11.7, 12.4, 13.8	many isobaric peaks	**1155.271**, 867.209, 865.194, 579.147, 577.132, 427.100, 425.084, 409.090, 407.074, 291.085, 289.070	9.2 *(**)*
c-tetramer-1-galloc (**Figure SI 14**)	1	1169.2546	-0.9	1191.3935	2.5	3.4	traces at higher r.t. (possible a-type tetramers)	**1169.255**, 1153.557, 881.192, 713.146, 699.867, 669.031, 633.061, 575.116, 476.465, 425.086, 409.092, 407.076, 325.112, 289.070, 247.060	2.5
l-tetramer-1-galloc (**Figure SI 15**)	> 10	1171.2710	-0.2	1193.4042	5.34, 6.36, 7.1, 7.4, 7.7, 8.0, 8.7, 9.3, 9.5, 9.9, 10.7, 11.3, 12.4, 12.7, 13.7, 14.2, 15.5, 16.2 (…)	7.5, 7.6, 7.9, 8.0, 8.7, 9.1, 9.2, 9.4, 10.5, 10.8, 11.9	many isobaric peaks	**1171.272**, 1155.274, 883.205, 867.212, 715.163, 697.154, 695.137, 679.144, 595.143, 593.127, 579.148, 577.133, 451.102, 427.101, 425.086, 409.091, 407.075, 397.091, 331.081, 305.064, 303.086, 301.070, 291.085, 289.070, 287.054, 275.054, 271.060, 265.143, 247.060	7.7 *(**)*
l-tetramer-2-galloc (**Figure SI 16**)	> 10	1187.2660	-0.2	1210.4107	2.0, 4.3, 4.4, 5.3, 5.9, 6.7, 6.9, 7.4, 8.4, 8.6, 9.0, 9.5, 9.9, 10.4, 10.9, 11.7, 12.8 (…)	2.2, 4.6, 6.5, 8.3, 9.0, 9.3, 9.6, 9.9, 20.8	many isobaric peaks	**1187.257**, 1171.257, 1003.376, 899.198, 883.198, 713.145, 595.139, 593.128, 577.129, 575.115, 529.730, 467.095, 425.084, 305.063, 289.070, 287.054, 247.059, 245.042	6.5
l-tetramer-3-galloc (**Figure SI 17**)	> 10	1203.2605	-0.4	1227.4120	3.1, 3.2, 4.1, 4.3, 4.7, 4.8, 5.3, 5.4, 6.0, 6.7, 6.9, 8.1 (…)	8.5, 8.7, 11.2, 15.5, 19.2, 19.7, 22.6	many isobaric peaks	**1203.2665**, 1187.2515, 852.9647, 690.5331, 609.1212, 595.144, 593.126, 437.298, 386.355, 329.992, 305.064, 291.086, 289.070, 287.054, 247.060	5.4 *(**)*
c-pentamer *(****)*	1	1441.3213	-2.0	1467.4863	4.3	5.8	traces at higher r.t. (possible a-type pentamers)	**1441.317**, 1423.306, 1289.270, 1271.260, 1263.249, 119.214, 1083.193, 967.167, 695.136, 577.132, 409.090, 407.074, 289.070, 247.060	4.3
l-pentamer	> 10	1443.3392	-0.5	1469.4974	6.9, 9.1, 9.9, 10.8,	6.0	many isobaric peaks	**1443.333**, 1425.322, 1291.289, 1155.273, 985.215,	9.9 *(**)*

(****)					11.6, 12.1, 13.2, 13.7, 14.5, 15.5 (…)			867.209, 865.194, 713.148, 695.137, 677.128, 579.149, 577.132, 559.121, 451.101, 425.085, 409.090, 407.075, 397.091, 291.085, 289.070, 247.060, 245.043	
c-pentamer-1-galloc (**Figure SI 20**)	1	1457.3181	-0.7	1484.4891	2.8	4.0	traces at higher r.t. (possible a-type pentamers)	**1457.315**, 1439.304, 1305.271, 1289.271, 1117.197, 947.173, 849.702, 577.134, 449.087, 425.087, 408.070, 407.076, 305.203, 289.071, 287.055, 271.060, 247.060	2.8
l-pentamer-1-galloc (**Figure SI 20**)	> 10	1459.3343	-0.3	1486.4995	4.3, 4.8, 5.5, 6.6, 7.3, 8.5, 9.4, 9.9, 10.3, 11.2, 12.3, 12.6, 13.6, 13.7, 14.3, 14.6, 15.0 (…)	3.7, 4.0, 4.9, 5.0	many isobaric peaks	**1459.332**, 1443.334, 1291.269, 1171.273, 1155.272, 883.203, 867.210, 865.193, 715.162, 593.127, 579.148, 577.132, 559.121, 467.096, 451.101, 449.085, 437.084, 427.102, 425.085, 409.090, 407.075, 331.080, 305.065, 301.070, 291.085, 289.070, 287.054, 275.054, 271.059, 247.060, 245.043	10.0 *(**)*
l-pentamer-2-galloc (**Figure SI 21**)	> 10	1475.3297	0.0	1503.4998	2.1, 4.6, 5.3, 5.8, 6.6, 6.9, 7.1, 7.4, 8.2, 8.5, 8.8, 9.1, 9.3, 9.6, 10.6, 10.9, 11.4, 12.4, 12.8, 13.1, 13.4, 13.6, 14.3 (…)	2.4, 2.5, 2.7, 2.9, 3.1, 3.2, 3.4, 3.7	many isobaric peaks	**1475.329**, 1459.329, 1313.306, 1187.259, 1171.267, 1155.269, 1043.235, 883.203, 881.185, 867.209, 595.142, 593.127, 579.148, 577.132, 575.114, 451.100, 427.010, 425.084, 409.090, 407.074, 305.064, 289.070, 287.054, 275.053, 271.059, 263.054, 247.059, 245.043	9.0 *(**)*
c-hexamer *(****)*	1	1729.3870	-0.2	NA	10.0	NA	weak	**1729.381**, 1711.365, 1577.334, 1559.325, 1441.316, 1289.269, 1119.211, 865.197, 695.136, 577.132, 559.123, 517.111, 409.090, 331.080, 289.070, 247.060	10.0
l-hexamer *(****)*	>10	1731.4010	-1.3	1762.5906	7.4, 8.0, 8.5, 9.5, 9.9, 10.1, 10.8, 11.3, 12.1, 12.6, 12.7, 13.5, 14.2, 14.7, 15.2, 15.5, 16.2, 17.0, 17.3, 18.4,	11.5, 11.6, 11.7, 11.8, 16.3	many isobaric peaks	**1731.402**, 1579.254, 1443.335, 1441.318, 1423.328, 1155.272, 1153.260, 867.210, 865.194, 697.152, 579.149, 577.131, 559.122, 451.102, 425.085, 331.079, 291.085, 289.070, 287.055, 271.059, 247.059	11.3 *(**)*

19.3 (…)

(*) ABBREVIATION USED: l = non-cyclic B-type oligomer, c = cyclic B-type, *n*a = A-type (where *n* = number of A-linkages) oligomer, CH3 = *O*-CH_3 substitution, afz = (epi)afzelechin, galloc = (epi)gallocatechin, gallate = gallate containing oligomer. “Dimer”, “trimer”, “tetramer”, “pentamer” and “hexamer” terms indicates the number of monomer units as mere (epi)catechins if not followed by any other indication; the subsequent text indicates the constituent monomers substitution and their number (substitutions on the (epi)catechin basic units); for example, 4-CH3 means that 4 OH groups are replaced by 4-OCH_3, 4-gallate means that 4 monomers are gallate esters, 4-afz means that 4 monomers are (epi)afzelechin units, *et cetera* (examples: l-dimer = B-type dimer with (epi)catechins only; a-dimer-1-gallate-1-galloc = A-type dimer with one (epi)gallocatechin and one (epi)catechin gallate, c-tetramer-2-galloc = cyclic B-type tetramer in which two monomers are (epi)gallocatechins). (**) arbitrarily taken at the highest peak of all isobaric TIC (MS/MS filter) peaks. (***) due to the decreased relative abundance in D_2O, fewer peaks were often detected than with H_2O. **(****)** see [11]. (*****) acquired at +3.8 kV.

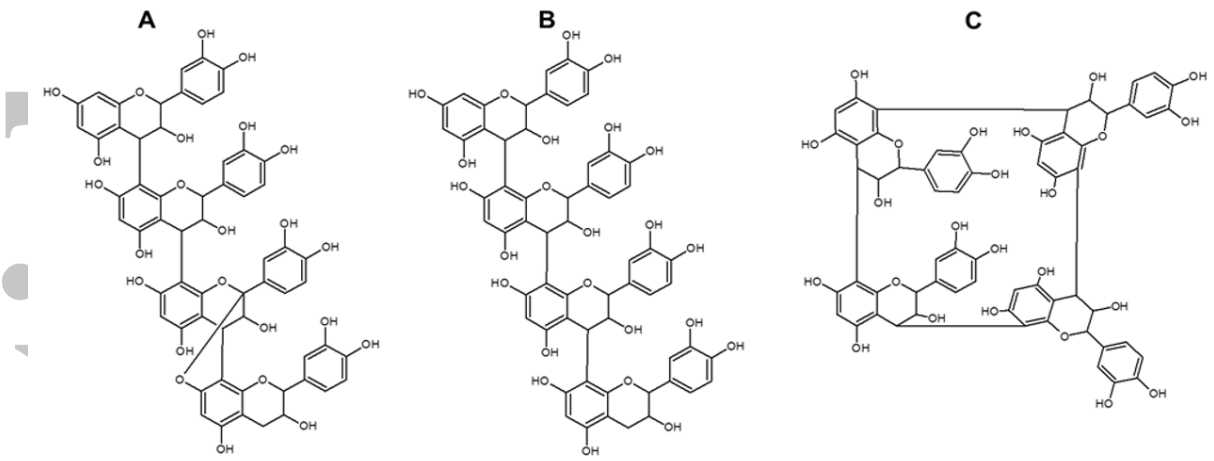

Figure 1. Example of tetrameric procyanidins. A) Linear tetrameric PC-A ($C_{60}H_{48}O_{24}$); B) Linear tetrameric PC-B ($C_{60}H_{50}O_{24}$); C) Cyclic tetrameric PC-B ($C_{60}H_{48}O_{24}$). The stereogenic centers' configurations and the arylic substitutions corresponding to the C-C inter-monomer linkages are to be considered undefined (e.g. *C4-C6* or *C4-C8* bonding) since they were not directly studied or discussed in this work.

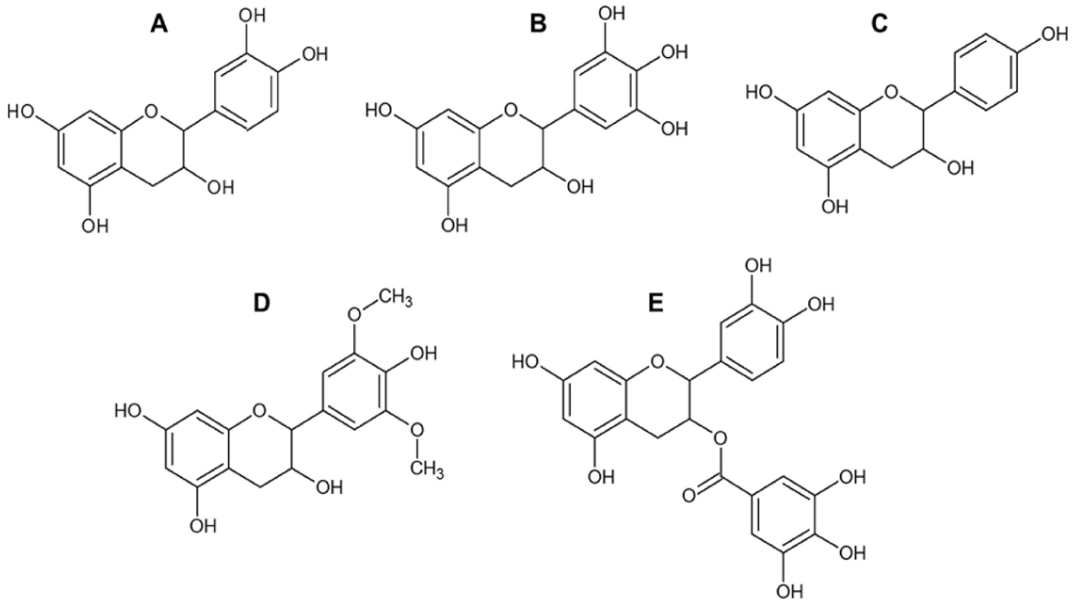

Figure 2. Examples of possible flavan-3-ol monomer units. A) (epi)catechin, B) (epi)gallocatechin, C) (epi)afzelechin, D) 3,5-*O*-dimethyl-(epi)gallocatechin, E) (epi)catechin gallate. The stereogenic centres configurations are not explicitly drawn since they are not directly taken into account in this report.

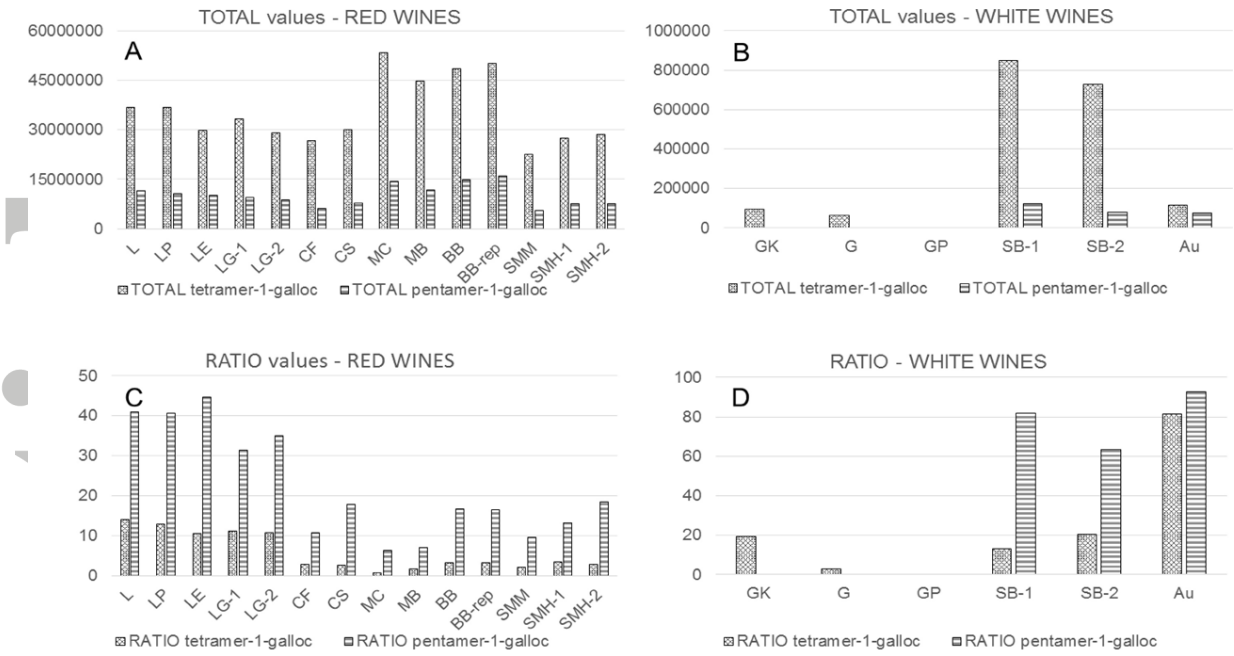

Figure 3. A) Sum of relative abundances for cyclic and non-cyclic tetramer-1-galloc, B) sum of relative abundances for cyclic and non-cyclic pentamer-1-galloc, C) ratios of abundances for c-tetramer-1-galloc over all tetramer-1-galloc, D) ratios of abundances for c- pentamer-1-galloc over all pentamer-1-galloc. The raw data are reported in **Table SI 2** (**Supporting Information**).

Legend: L = Lagrein, LP = Lagrein Prestige, LE = Lagrein Eyrl, LG = Lagrein Grieser, CF = Cabernet Franc, CS = Cabernet Sauvignon, MC = Merlot collection, MB = Merlot barrique, BB = Blauburgunder, SMM = St.Magdalener Moar, SMH-1 = St.Magdalener Huck-1, SMH-2 = St.Magdalener Huck-2, GK = Gewürztraminer Kleinstein, G = Gewürztraminer, GP = Gewürztraminer Passito, SB-1 = Sauvignon blanc-1, SB-2 = Sauvignon blanc-2, Cp = Chardonnay Passito 'Aurum'.